AFRL-RI-RS-TR-2020-093

DDARING: DYNAMIC DATA-AWARE RECONFIGURATION, INTEGRATION AND GENERATION

GEORGIA TECH RESEARCH CORPORATION

JUNE 2020

FINAL TECHNICAL REPORT

APPROVED FOR PUBLIC RELEASE; DISTRIBUTION UNLIMITED

STINFO COPY

AIR FORCE RESEARCH LABORATORY
INFORMATION DIRECTORATE

■ **AIR FORCE MATERIEL COMMAND** ■ **UNITED STATES AIR FORCE** ■ **ROME, NY 13441**

NOTICE AND SIGNATURE PAGE

Using Government drawings, specifications, or other data included in this document for any purpose other than Government procurement does not in any way obligate the U.S. Government. The fact that the Government formulated or supplied the drawings, specifications, or other data does not license the holder or any other person or corporation; or convey any rights or permission to manufacture, use, or sell any patented invention that may relate to them.

This report is the result of contracted fundamental research deemed exempt from public affairs security and policy review in accordance with SAF/AQR memorandum dated 10 Dec 08 and AFRL/CA policy clarification memorandum dated 16 Jan 09. This report is available to the general public, including foreign nations. Copies may be obtained from the Defense Technical Information Center (DTIC) (http://www.dtic.mil).

AFRL-RI-RS-TR-2020-093 HAS BEEN REVIEWED AND IS APPROVED FOR PUBLICATION IN ACCORDANCE WITH ASSIGNED DISTRIBUTION STATEMENT.

FOR THE CHIEF ENGINEER:

/ S /
UTTAM MAJUMDER
Work Unit Manager

/ S /
GREGORY HADYNSKI
Assistant Technical Advisor
Computing & Communications Division
Information Directorate

This report is published in the interest of scientific and technical information exchange, and its publication does not constitute the Government's approval or disapproval of its ideas or findings.

REPORT DOCUMENTATION PAGE

Form Approved
OMB No. 0704-0188

1. REPORT DATE *(DD-MM-YYYY)*	2. REPORT TYPE	3. DATES COVERED *(From - To)*
JUNE 2020	FINAL TECHNICAL REPORT	SEP 2014 – DEC 2019

4. TITLE AND SUBTITLE

DDARING: DYNAMIC DATA-AWARE RECONFIGURATION, INTEGRATION AND GENERATION

5a. CONTRACT NUMBER
FA8750-18-2-0108

5b. GRANT NUMBER
N/A

5c. PROGRAM ELEMENT NUMBER
62716E

6. AUTHOR(S)

Vivek Sarkar

5d. PROJECT NUMBER
SDH1

5e. TASK NUMBER
GT

5f. WORK UNIT NUMBER
EC

7. PERFORMING ORGANIZATION NAME(S) AND ADDRESS(ES)
GEORGIA TECH RESEARCH CORPORATION
505 10th ST NW
Atlanta GA 30332

8. PERFORMING ORGANIZATION REPORT NUMBER

9. SPONSORING/MONITORING AGENCY NAME(S) AND ADDRESS(ES)

Air Force Research Laboratory/RITB
525 Brooks Road
Rome NY 13441-4505

10. SPONSOR/MONITOR'S ACRONYM(S)
AFRL/RI

11. SPONSOR/MONITOR'S REPORT NUMBER
AFRL-RI-RS-TR-2020-093

12. DISTRIBUTION AVAILABILITY STATEMENT
Approved for Public Release; Distribution Unlimited. This report is the result of contracted fundamental research deemed exempt from public affairs security and policy review in accordance with SAF/AQR memorandum dated 10 Dec 08 and AFRL/CA policy clarification memorandum dated 16 Jan 09.

13. SUPPLEMENTARY NOTES

14. ABSTRACT

The DDARING TA2 project has created software technologies that advances the SDH program goals by developing a novel programming system for generating optimized code variants and optimized hardware configurations for TA1 hardware platforms. Our approach is capable of accelerating workflows for data-intensive analyses to achieve near-ASIC performance, but with the productivity that analysts have come to expect from modern problem-solving environments such as Julia and Python.

15. SUBJECT TERMS

Code optimization, Knowledge base, Machine learning, Multi-version code generation, Python.

16. SECURITY CLASSIFICATION OF:			17. LIMITATION OF ABSTRACT	18. NUMBER OF PAGES	19a. NAME OF RESPONSIBLE PERSON
a. REPORT	b. ABSTRACT	c. THIS PAGE			**UTTAM MAJUMDER**
U	U	U	UU	33	19b. TELEPHONE NUMBER (*Include area code*) **N/A**

Contents

List of Figures

List of Tables

1 Executive Summary

DARPA's program on "Software Defined Hardware" (SDH) put forth a grand challenge to build runtime-reconfigurable hardware (TA1) and software (TA2) that enables near ASIC performance without sacrificing programmability for data-intensive algorithms. As a TA2 performer, the DDARING team addressed this challenge in Phase 1 of the SDH program by introducing multiple software innovations for future hardware with programmability that is comparable to what data scientists expect today. The results of our research have been published in 16 peer-reviewed publications [1–16]. As described in these publications, and in this report, the main advances have been in the following areas:

1. As described in Section 3.1, we designed and implemented a new Python-based programming model, called Intrepydd, that is suitable for ahead-of-time compilation. Depending on the mode selected during compilation, code generated from Intrepydd programs can be integrated within a Python application, or a C++ application. The first mode was used by testers in the Phase 1 programmability evaluations who were given access to the Intrepydd v0.2 toolchain via a docker container, and the second mode was used to enable code generation for the simulator developed by our TA1 partner (which does not support a Python runtime environment).

2. We also designed and implemented the first version of the DDARING knowledge base, summarized in Section 3.2, with the goal of learning and storing extensive information on (a) mapping of workflow "steps" to "kernels", and (b) mapping of kernels to available hardware configurations.

3. Section 3.3 summarizes our work in Phase 1 on static code optimizations. The approaches that we have taken to multi-version code generation promises to advance state of the art in data-aware code optimization, as demonstrated in our results for the Word2Vec workflow and data clustering workflows.

4. Section 3.4 summarizes our early work on extending the foundations of dynamic code optimization, with demonstrations of opportunities for automatic tuning of floating-point precision in deep learning workflows as well as reduction of fixed-point precision in important integer applications.

5. Finally, Section 3.5 summarizes the advances that we have made in using various machine learning techniques for key tasks that need to be performed by an online auto-tuner, including identifying the application domain of the currently executing kernel, detection of a phase change in execution characteristics, and selection of optimized code and hardware configurations.

Our results show that the DDARING programming system has made significant progress towards the SDH program goals in Phase 1. The programmability of the Intrepydd tool chain is already close to that of Python. Further, our toolchain, in Phase 1, has already bridged a large fraction of the typical orders-of-magnitude gap between Python and theoretical peak performance. In Section 4.1, we used the "surrogate model" approach to approximately estimate execution time, energy and GOPS/Watt metrics on SDH hardware for Intrepydd

and Python implementations. The performance evaluations using the surrogate model showed 130.2× geometric mean speedup and 314.1× geometric mean energy efficiency by the Intrepydd implementations, compared with the Python implementations.

Further, the performance evaluations on dual Intel Xeon Silver 4114 CPUs with 10 physical cores per CPU socket were performed. We compare the single-core performance of Python, Cython, Numba, unoptimized INTREPYDD, and optimized INTREPYDD for six SDH workflows that span different data science domains summarized in Table 2. One of these benchmarks was chosen because it is dominated by native library calls in its execution time, and the other five are non-library-dominated benchmarks. As shown in Figure 19, the optimized INTREPYDD version in `host=python` mode shows performance improvements in the range of 11.1× to 8809.8× for the five non-library-dominated benchmarks, and of 1.5× for the library-dominated benchmark, compared to baseline Python. Similarly, the optimized INTREPYDD in `host=python` mode shows 1.5× - 50.5× of performance improvements over existing state-of-the-art techniques, Cython and Numba. We also evaluated the parallel performance for four of the six benchmarks that were candidates for using INTREPYDD's `pfor` construct, on a dual socket Intel Xeon E-2680 V4 (14 cores per socket). As shown in Figure 20, the optimized INTREPYDD in `host=cpp` mode shows 2.0× - 8.0× speedups using 16 cores, with respect to the sequential optimized INTREPYDD.

2 Introduction

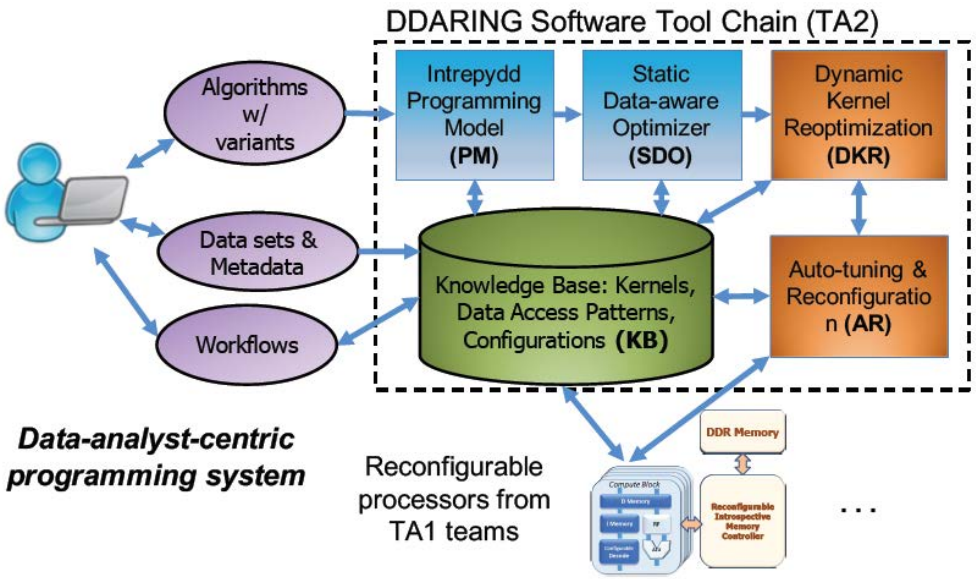

Figure 1: Overview of DDARING programming system.

As a TA2 effort, the DDARING project aims to advance the SDH program goals by developing a novel programming system for generating optimized code variants and optimized hardware configurations for TA1 hardware platforms. Figure 1 shows an overview of our technical approach with the overall goal of accelerating workflows for data-intensive analyses

to achieve near-ASIC performance, but with the productivity that analysts have come to expect from modern problem-solving environments such as Julia and Python. As illustrated in Figure 1 and described below, we have developed in Phase 1 a new high-level programming model (Section 3.1), a knowledge base (Section 3.2), a static data-aware optimizer (Section 3.3), a dynamic kernel reoptimizer (Section 3.4), and an auto-tuning and reconfiguration system (Section 3.5).

3 Methods, Assumptions and Procedures

3.1 Intrepydd Programming Model

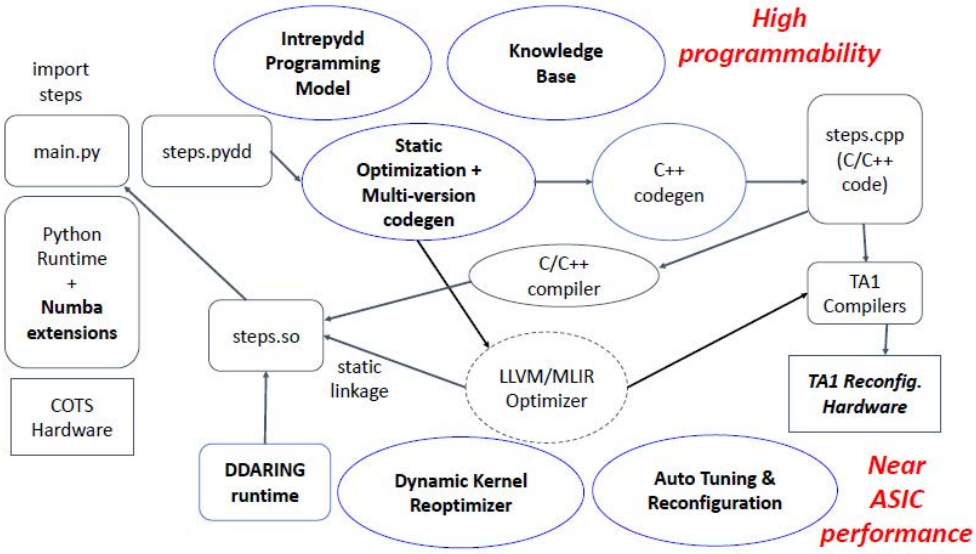

Figure 2: Design of Intrepydd tool chain for `-host=python` mode

Intrepydd is a new analyst-friendly Python-based programming model suitable for ahead-of-time (AOT) compilation on current and future hardware platforms and accelerators, thereby enabling "performance programming" in a lightweight Python syntax. It builds on an AOT-compilable subset of Python with extensions for matrix, tensor, graph, and deep learning computations that expose opportunities for dynamic data-aware code optimizations and hardware reconfiguration.

Intrepydd is not intended for writing complete/main programs. Instead, code generated from Intrepydd programs can be integrated within a Python application (with the `-host=python` mode) or within a C++ application (with the `-host=cpp` mode). Intrepydd was designed from scratch for the SDH program. Figure 2 summarizes the design of the Intrepydd tool chain for `-host=python` mode.

We released v0.2 of Intrepydd in end-May for use in the Phase 1 programmability evaluation and developed v0.3 after that as the latest version used to obtain the Phase 1 evaluation results presented later in this report. A list of v0.2 features is summarized below, followed by a summary of the extensions in v0.3.

3.1.1 Summary of Intrepydd v0.2 features

Intrepydd v0.2 only supports the `-host=python` mode, and encourages incremental use of Intrepydd within a familiar Python ecosystem, including Jupyter notebooks and standard Python profiling tools. A programmer creates an Intrepydd module in a file with a `.pydd` extensions, and invokes the Intrepydd compiler, `pyddc`, to enable AOT compilation. A key requirement in Intrepydd v0.2 is that all function parameters and return values must be declared with explicit types. Intrepydd code can be invoked from Python by importing the Intrepydd module, similar to importing a Python module. Examples of Intrepydd code are provided in Section 4.3.

Intrepydd v0.2 supports `bool`, `int32`, `int64`, `float32`, and `float64` as primitive types, as well as dense arrays, sparse arrays, and lists of primitive types. These data types are inferred automatically for local variables and expressions, based on the type declarations provided for parameters and return values. In some cases, explicit type declarations may be needed for assignment statements by using Python's PEP 484 type annotation with the "var: Type" syntax. Support for other type annotations, e.g., PEP 526, is deferred to future versions of Intrepydd.

Intrepydd v0.2 also supports the following standard statement types from Python: assignment statements, function calls, return statements, sequential for and while loops with break / continue statements, and conditional if/elif/else statements. In addition, Intrepydd v0.2 supports a parallel for (pfor) loop statement, which is not available in Python. Intrepydd expressions can be constructed using a large set of unary and binary operators on scalars and arrays, as well as list constructors and array element operators.

There are some documented syntactic limitations in v0.2 of Intrepydd, which will be addressed in future releases. Certain Python array operators need to be replaced by alternate Intrepydd function calls in v0.2, e.g., + → add(), / → div(), * → mul(), @ → matmult() or spmm(), len(x) → x.shape(0), a:b → range(a,b). In addition, NumPy calls need to be replaced by generic calls so that it is possible to compile Intrepydd code with no NumPy dependencies in the `-host=cpp` mode, e.g., np.zeros() → zeros(), np.sqrt() → sqrt(). Finally, some currently unsupported Python calls have to be replaced by explicit code, e.g., sum(axis=...) → reduction loop, append() → append loop, maximum() → code to compute max, and replacement of an unsupported allocation function by a call to a supported allocation function followed by updates to the allocated array.

3.1.2 Summary of Intrepydd v0.3 extensions

The Intrepydd v0.3 implementation extends Intrepydd v0.2 with the following features: addition of `SparseMat` as a builtin type for sparse matrices, enhanced type inference so that function return types can be automatically inferred, removal of some of the syntactic limitations in v0.2, improved error messages from the `pyddc` compiler, and command-line options such as specifying compiler/linker flags. Further, a new loop invariant code motion (LICM) optimization was added that can also be applied to array operators, instead of just scalar operators as in traditional compiler implementations of LICM. Finally, a number of additional built-in wrappers were added for popular libraries for arrays including: where(), element-wise logical and max operations, sparse array creation from dense vectors,

sum(axis=...) reduction on an axis, and builtin support for the heap data structure.

3.2 Knowledge Base

The goal of the knowledge base is to enable the acceleration of workflows by storing and learning extensive information on (a) mapping of workflow "steps" to "kernels", and (b) mapping of kernels to available hardware configurations.

Representation

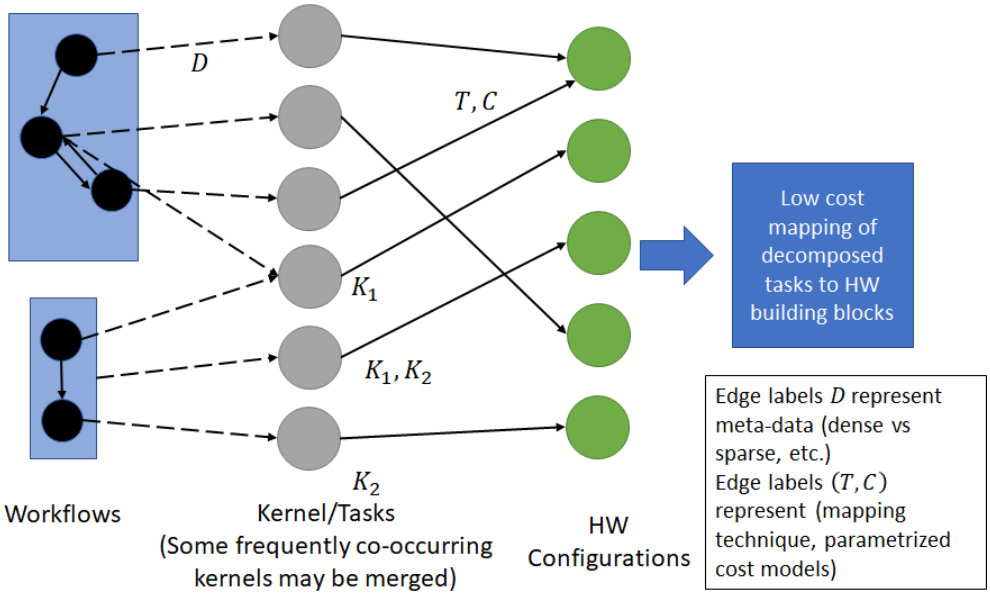

Figure 3: Tripartite Representation of Knowledge Base

The knowledge base comprises of a rich tripartite graph representation $G(V_1, V_2, V_3, E)$ (TGR) as shown in figure 3. The first layer V_1 consists of Domain-Specific Language level (DSL) steps. A step is a pattern of computation that can be mapped to one or a combination of kernels. The set V_1 is the steps discovered in a codebase which includes a wide range of data-intensive workflows. Each $u \in V_1$ is attributed with a feature D to quantitatively represent computational and data access patterns of the step (or part of the workflow) such as access pattern irregularity, data precision, computation to communication ratio, etc. A workflow is a finite-state-machine of the steps in V_1. Nodes in set V_2 represent bare bone tasks or kernels that form the core of the knowledge base. A step may have multiple variants in terms of kernels. For instance, a convolution operation can be represented as 1) a sequence of frequency domain transformation, multiplication and inverse transformation steps, or 2) a series of sliding window dot products. Frequently co-occurring kernels may be merged to form one kernel for optimized implementations. The kernels $K \in V_2$ are mapped to the underlying building blocks of the hardware platform. The hardware configurations and building blocks are represented as vertices $v \in V_3$. Note that a kernel can be mapped to one hardware configuration $(\mathcal{T}, C)$ in multiple ways $(\mathcal{T})$ with different performance costs (C). This is

desirable as it would provide ways to schedule a task even if the optimal hardware block for execution is busy. Vertices in V_3 also store their cost of reconfiguration, which is taken into account while computing the optimal mapping and overall cost of kernel execution. We have partially populated the knowledge base using execution profiles from SDH workflows.

Learning Kernel-to-Hardware Performance Models

The performance models are designed to be trained on the target hardware. We want these models to be small so that when the knowledge base is bootstrapped on a new machine, it can run some benchmarks to train performance models for a set of kernels quickly. Currently, we have built prediction models for three operations: Matrix-Matrix Multiplication, Matrix-Vector Multiplication, and Convolution. We perform the modeling for each of these kernels, and then train it on the desired hardware. For a given kernel, the model remains fixed, while the parameters, i.e., the weights differ over different hardware. Our model is a compact neural network, augmented with mathematical formulae for complexity for the kernel, for e.g., $Cn_1n_2n_3$ for multiplying matrices of size $n_1 \times n_2$ and $n_2 \times n_3$; C is a constant learned through training. Overall the number of parameters are kept under 75 and training is performed with 250 samples only for each kernel-hardware pair to ensure small memory footprint and fast training. The models only take input dimensions and matrix densities as input and output the predicted runtime. Table 1 shows the prediction results from our approach[1]. Our approach significantly outperforms baselines, including neural networks (without complexity augmentation) and linear regression. We also obtained up to 1.3× higher accuracy with larger models ($\sim$ 1000 parameters) and larger data ($\sim$10000 samples) but have omitted the results as they are not practical due to slow training and large memory requirement.

Table 1: Runtime prediction results for top three SDH kernels – Mean Absolute Error (Mean Absolute Percentage Error), Training Time.

Operation	Intel(R) Core i7-8750H CPU @ 2.20GHz	Intel(R) Core i5 CPU @ 2.30GHz	Intel(R) Xeon(R) CPU E5-2650 v2 @ 2.60GHz	Tesla K40c	Quadro K420
Matrix-Matrix	0.06s (30.35%) 3min	0.06s (21.75%) 3min30s	0.04s (25.85%) 2min30s	$2.36 * 10^{-4}$s (14.95%) 10.76s	$2.36 * 10^{-4}$s (9.72%) 10.56s
Matrix-Vector	$2.76 * 10^{-4}$s (12.32%) 2min	$7.52 * 10^{-4}s$ (19.81%) 2min	$4.25 * 10^{-4}$s (8.03%) 2min	$1.15 * 10^{-5}s$ (7.00%) 7.31s	$1.22 * 10^{-5}$s (7.96%) 7.79s
Convolution	0.05s (24.88%) 2min30s	0.02s (10.51%) 2min30s	0.04s (12.26%) 4min	7.79*10-5s (9.63%) 15s	$1.22 * 10^{-4}$s (15.07%) 13.7s

[1]While Section 4 presents and discusses detailed end-to-end results for our approach, we also include some per-component results in Section 3 to aid in the presentation of methods, assumptions and procedures.

3.3 Static Data-aware Optimizer

Our approach to static data-aware optimization is founded on multi-version code generation, which can have benefits in at least two ways: 1) generating specialized code for different classes of data inputs, and 2) selecting the best algorithmic strategy for a given data input. Below, we summarize our work on optimizing the Word2Vec workflow as an illustration of 1), and our work on optimizing data clustering workflows as an illustration of 2). Both optimization approaches are enabled by high-level semantic information in the Intrepydd programming model.

Code specialization for the Word2Vec workflow

Word2Vec is an SDH workflow, and an important kernel in Natural Language Processing (NLP). It is widely used to embed words from textual data in a vector space. Previous work improved the performance of the original Word2Vec implementation by converting vector-vector operations to matrix-matrix operations and using state-of-the-art BLAS routines for the resulting level-3 BLAS operations. This conversion effectively batches inputs and shares the same negative samples across a batch of inputs. However, many performance overheads remain in his approach because a) many of the matrix sizes have highly nonuniform aspect ratios that are not well suited to BLAS, e.g., tall and skinny matrices, and b) we make several library calls for consecutive operations, which reduces register reuse. These overheads motivate the generation of multi-version code for different matrix sizes. Our preliminary results show significant performance improvement over the state-of-the-art Word2Vec implementation on x86.

In our evaluation, we used the Skip-Gram with Negative Sampling (SGNS) for Word2Vec. We statically generated multi-version code specialized on two parameters - number of inputs and number of outputs - so that the appropriate specialized code can be chosen at runtime based on the parameter values for each call. Our evaluation was performed on the widely used Billion Word Language Model Benchmark, with a word vector length of 300, a window size of 5 (which implies that the number of inputs can vary from 1 to 10), and 5 negative samples (which implies that the number of outputs can vary from 1 to 6). This results in 60 possible combinations for the number of inputs, M, and the number of outputs, N. The specialized code generated by our system was observed to be $1.78\times$ to $5.71\times$ faster than the state of the art across all 60 combinations. The largest performance improvement of $5.71\times$ was observed for $(M, N) = (2, 4)$ and the smallest improvement of $1.78\times$ was observed for $(M, N) = (8, 6)$.

Algorithm selection in Data Clustering workflows

Going beyond code specialization, a higher-level optimization opportunity can be found in algorithm selection. For example, KMeans, DBSCAN, KNN, PCA are a few choices for data clustering algorithms. The ideal choice of algorithm can depend on the data input and the target hardware, and a poor choice can impact the accuracy or performance of the workflow. In this preliminary work, we sought to automate the selection of Kmeans vs. DBSCAN algorithms to solve data clustering problems with different inputs. The goal of our approach is to build an efficient library that automatically selects among KMeans and

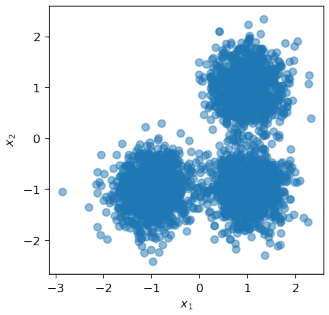

Figure 4: Original data distribution for dataset1

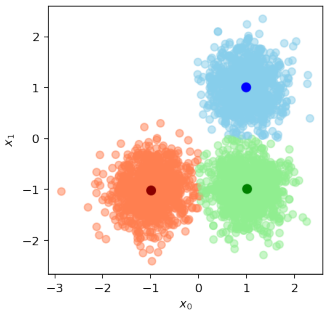

Figure 5: Results of KMeans

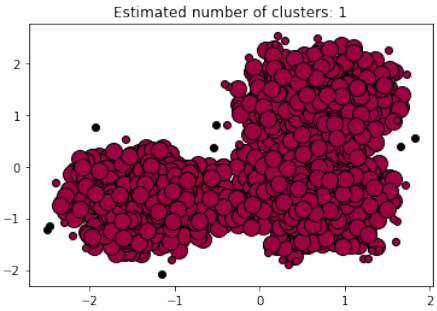

Figure 6: Results of DBSCAN

DBSCAN algorithms. To improve the effectiveness of the library, we adopt a sub-sampling method to choose between the two clustering algorithms; sub-sampling method reduces the cost of executing the two candidate clustering algorithms on a given data set. Currently, our library works with data sets containing two-dimensional data points.

Two data sets were used for testing the algorithm selection library and analyzing scenarios when one of the clustering algorithms would be better than the other one. Figure 4 shows the original data distribution of the given dataset, which dataset was generated using the scikit module. Our subsampling approach suggested that the Kmeans algorithm (Figure 5) would yield a better result than DBSCAN (Figure 6), thereby selecting the better algorithm with low overhead since subsampling was performed on a dataset that was 0.1% of the size of the actual input data set in Figure 4.

3.4 Dynamic Kernel Reoptimizer

Deep Neural Networks Training Precision Tuning

Researchers have shown that DNNs are able to preserve accuracy while operating with reduced precision data formats. Using narrow precision operations has two main benefits: (1) Reducing the number of memory accesses. (2) Increasing the throughput with SIMD-like operations. As a result, it is possible to gain energy savings and speedups by performing DNN computations in a narrow precision format. As the required bit-width varies among different networks and layers, a dynamic precision tuning system is needed in order to maximize savings while preserving the network's accuracy. Although both reduced precision training and inference are active fields of research, our main focus is on the training phase because it runs longer and is more compute and memory intensive than inference. In this report, first, we examine the potential benefits of narrow precision computation during the training. After that, we propose a design to tune a network's precision automatically during training while maintaining its accuracy.

Manual Precision Exploration:

In this section, we discuss our tool, which allows us to run the input network with a user-defined precision configuration (Figure 7). The user must declare the layer-wise network configuration before training. Once training is complete, the user can evaluate the trained network and reconfigure the precision if desired. By repeating this procedure, the user can

find the narrowest precision that preserves the accuracy of the network. It is possible to set an arbitrary precision for each layer, and this precision can vary among different epochs.

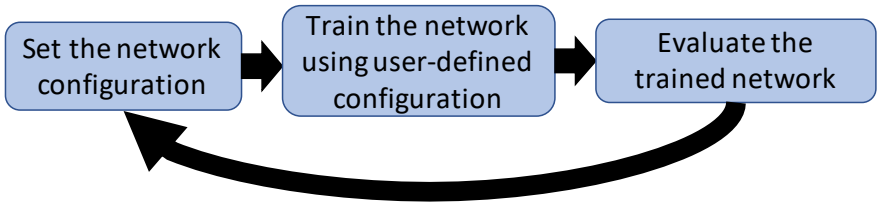

Figure 7: Manual system overview

The PyTorch framework does not support arbitrary precision operations. Thus, we had to add arbitrary precision computation capability to the framework. Each of PyTorch's three implementation layers had to be re-implemented. Figure 8 shows a high-level block diagram of the PyTorch extension. The first level is CUDA, which has all the computationally intensive kernels. The second one is the CPP Wrapper, which prepares the input data of the computation kernels. The last one is the PyTorch Frontend, which is a wrapper for the CPP code and provides the interface to the user. The CUDA kernels are able to perform computations in arbitrary precision.

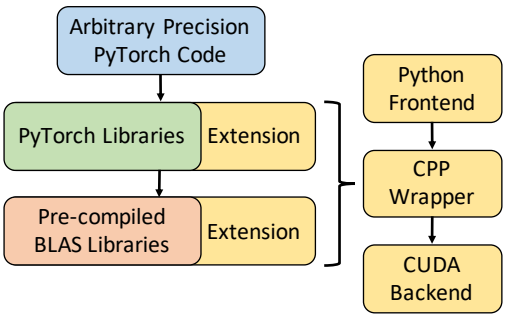

Figure 8: PyTorch extension

Using this tool, we were able to calculate potential savings in multiple benchmarks. Figure 9 compares the potential memory savings in three different scenarios. First, saving all the parameters in half float format, which does not guarantee the network's accuracy. Second, performing all the training using one precision for each layer of the network, named "Dynamic One Width". Third, finding the narrowest precision for each layer per epoch and dynamically changing the precision, named "Dynamic Multi Width". Dynamic One Width is not achievable as it needs to know the precision requirement of each layer during the training beforehand of starting the process. Our proposed idea is Dynamic Multi Width, which outperforms all the other methods.

Figure 10 compares the amount of computation required for the full precision and reduced precision formats, assuming that computational units are fully dynamic and are able to perform arbitrary precision.

These results are promising and motivate us to work on a tool that tunes the precision automatically.

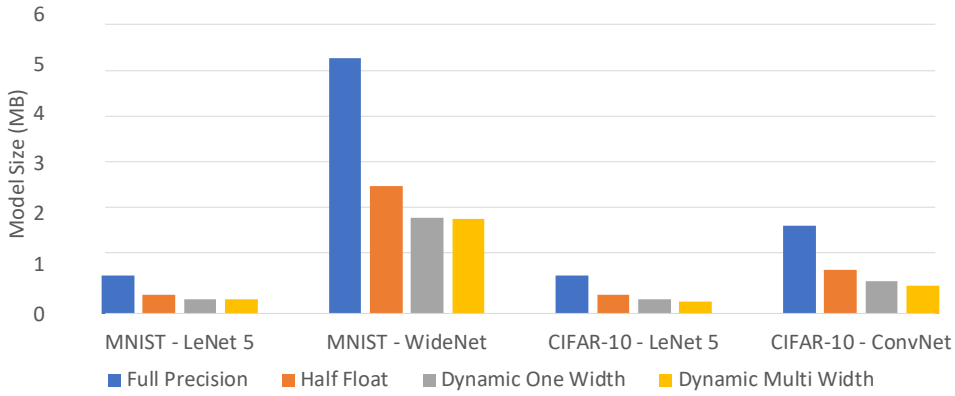

Figure 9: Potential memory savings

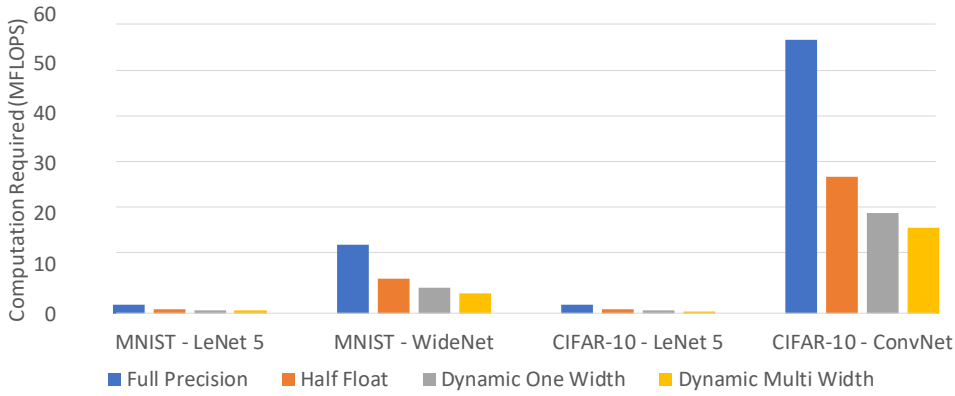

Figure 10: Potential compute savings

Dynamic Precision Reconfiguration:
As mentioned in the previous section, having an automatic tool that finds the best precision configuration while the training is going on is required in order to train arbitrary networks efficiently. Figure 11 shows an overview of the proposed system, which periodically reevaluates the best precision configuration for the network every few epochs of training. In this automatic system, the user has no role to play and retraining the network is not required.

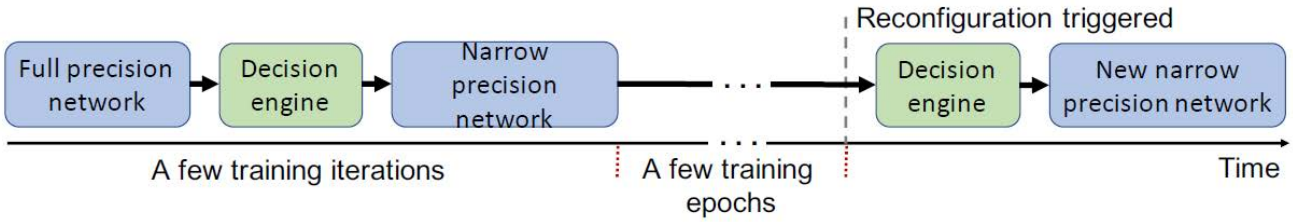

Figure 11: Overview of auto precision tuning system

Whenever precision reconfiguration is required, the decision engine (Figure 12) routine is called. The decision engine clones the original network to multiple candidate networks that have the potential to have the best precision configuration. After training all the networks

for a few iterations, the decision engine evaluates candidates based on different metrics (direction of weights update, the loss value, etc.) and finds the configuration which has the best precision. After that, the network will be trained with the chosen candidate configuration until the next time the decision engine is called. As wrong decisions from the decision engine might cause divergence during the training process, the system has a check-pointing based recovery strategy. This system is currently in progress.

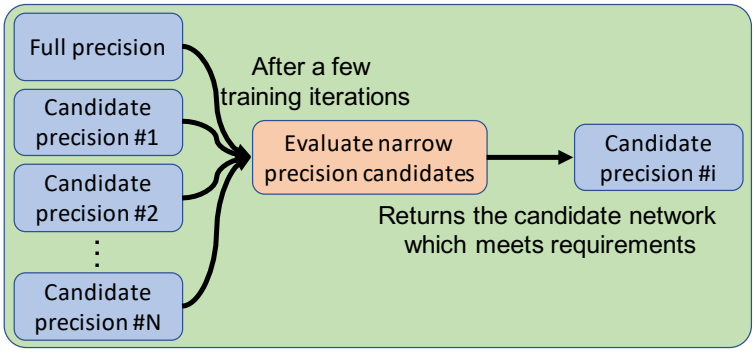

Figure 12: Decision engine overview

Integer Precision Reduction

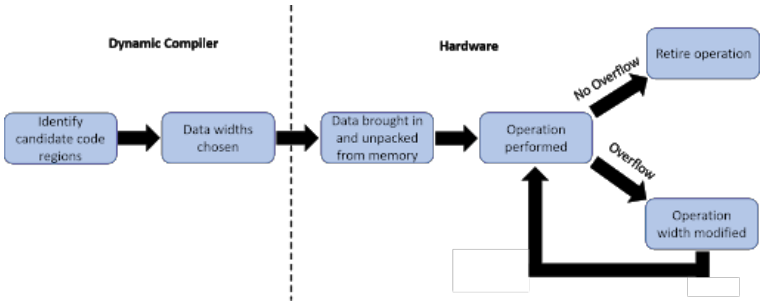

Figure 13: Integer precision system overview

As shown in Fig. 13, the dynamic integer precision reduction system has two components: the dynamic compiler and the hardware. The compiler will use profiling and application information from the knowledge base to decide on appropriate data widths for storage and operations. To reduce the overhead of the profiling step, the functionality could be added to identify code regions amenable to precision reduction, so values from the entire program do not have to be sampled.

The hardware will pack and unpack data from memory on loads and stores according to the compiler-chosen data width. This allows for potential savings in the memory system as fewer memory and cache accesses will be needed for the same amount of data. Once the data is in the register file, we can perform operations in the reduced width and recover if we are too aggressive. The key insight is that we can use the already existing overflow bit in modern processors to detect a data width violation in integer computation.

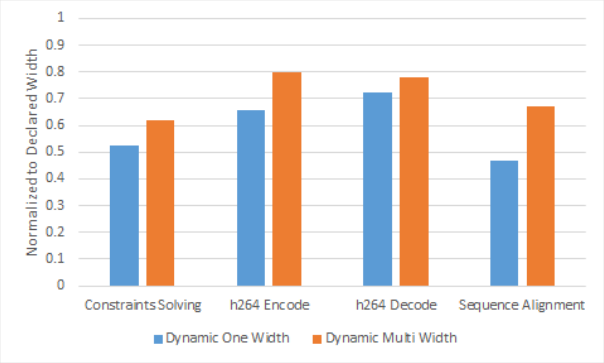

Figure 14: Opportunity for Data Width Savings

To motivate the dynamic integer precision reduction system, we see in Fig. 14 that four prominent integer applications: constraints solving (SAT), genomic sequencing, video encoding, and video decoding on average leave about 60% of their data widths unutilized. The Dynamic One-Width shows the potential data width savings if each instruction only uses its maximum required width over the course of execution, and the Dynamic Multi-Width shows potential savings if the instruction width could perfectly adapt to the needs of the data. Note that these two metrics are oracles and can only be found after processing is complete as precision is dependent on the input data. Based on these preliminary results, in Phase 2, our goal will be to evaluate the system and provide performance and energy results in simulation for existing hardware with minor modifications. The results will then be extended to hardware with fast reconfiguration times to showcase the additional gains that an SDH machine could provide.

3.5 Auto-tuning and Reconfiguration system

This section summarizes the advances that we have made in using various machine learning techniques for key tasks that need to be performed by an online auto-tuner, including identifying the application domain of the currently executing kernel and detection of a phase change in execution characteristics. Due to space limitations, we omitted text on our approach to the selection of optimized code and hardware configurations, which was also presented at the recent SDH PI meetings.

Application Domain Detection

In DDARING, we define the application domain as a group of programs that shares similar characteristics and serves a similar purpose. For example, matrix decomposition, such as LU, $Cholesky$, PDP^{-1}, are likely to be in the same application domain, since they consist of similar matrix manipulation operations and are all usually used for solving linear systems.

To identify the application domain of a given program, we first capture the behavior of the application by profiling and collecting data from performance counters in the processor's performance monitoring unit (PMU). We then use a Long Short-Term Memory (LSTM) classifier that operates on sequences of PMU data collected from a real machine. In the

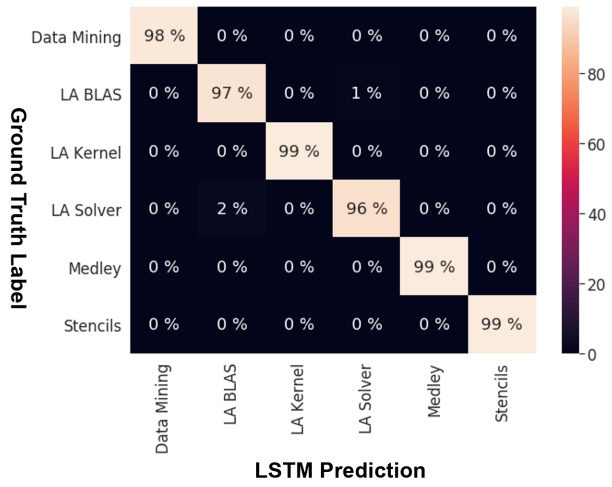

Figure 15: Error matrix of the test set constructed with seen applications

following subsections, we will describe the data we collected, how we process the raw data to create a dataset, and how we train and evaluate the LSTM model.

Data Acquisition and Pre-processing:

To collect all the raw data from the performance counters, we utilized the *perf* tool on Linux distributions. The processor in the test system that we used is an Intel CPU with 53 performance counters available. Due to the limitation of the processor and the profiling tool, we were not able to collect all the values at once, so we have to collect only 5-7 counters at a time, and use time multiplexing to collect all counter values. We used a sampling interval of 100ms due to system limitations, but we assume that the target SDH hardware will be able to support much higher sampling rates.

Model Construction and Training:

LSTM is a type of recurrent neural network (RNN) that specializes in detecting long-term relationships of sequential data. It has shown impressive performance on a variety of tasks such as speech-recognition and neural machine translation. Since the classification of sequences of performance data is conceptually similar to these tasks, we believe that LSTMs will work well for our purpose.

We implemented the LSTM with the popular PyTorch framework with the help of scikit-learn and Numpy on preprocessing and dataset construction. Since one of the main requirements of the application domain detection, in the context of DDARING, is to detect the domain without large run-time overhead, we limited the size of the neural network for faster inference and lower resource consumption. Our final model consists of a single layer LSTM with 128 hidden units, and a single classification layer for generating the final classification.

For this evaluation, the number of output classes is 6, and correspond to the application classes identified in [17]. In the future, we plan to expand the application classes for increased coverage of SDH workflows. For simplicity, we use regular stochastic gradient descent for training and set the learning rate to 0.01 for faster convergence. In our experiments, we didn't observe significant over- or under-fitting. We did the training and evaluation with an Nvidia GTX1080 GPU, and the model is trained for 35 epochs, which takes around 5

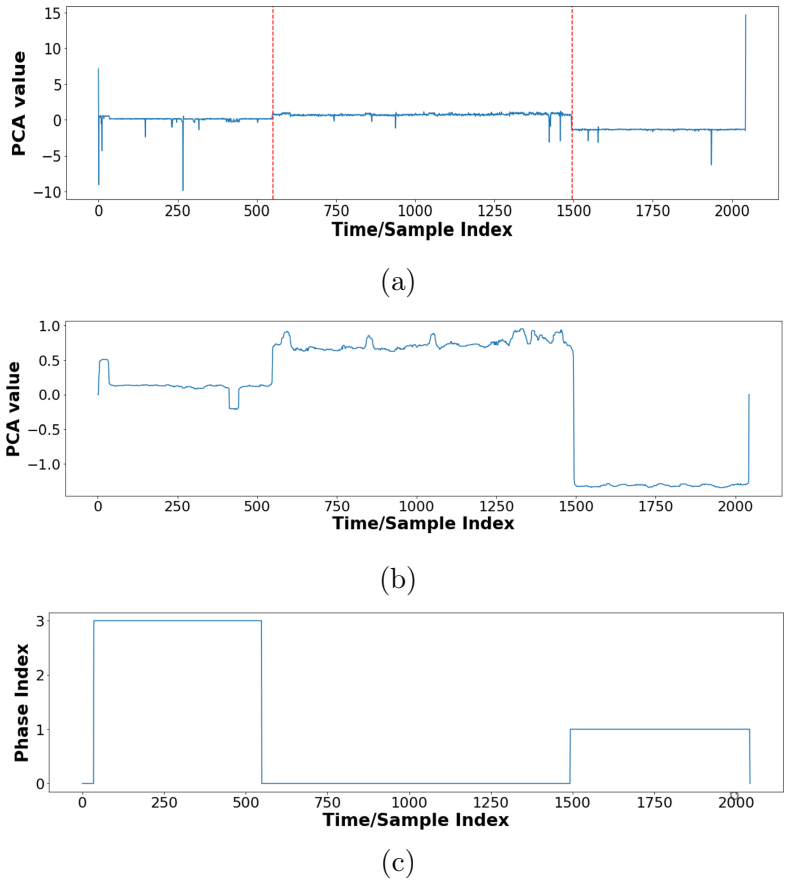

Figure 16: Output from different stages of phase detection

minutes. Note that the time might vary depending on the system configuration and the code implementation.

Evaluation and Results:

The results show that on the test set, the LSTM can correctly classify 98% of the sequences. The error matrix presented in Figure 15 shows that it can correctly classify 99% of the sequences from most of the domains. The only non-zero entries occur for linear algebra classes that exhibit similar characteristics (LA BLAS and LA Solver).

Program Phase Detection

Dynamic reconfiguration is one of the most important features of DDARING. In reality, the applications can have multiple program phases, in which the performance and behavior of the system are relatively steady. During these periods, the system can be reconfigured to adapt to the characteristics of the phase to achieve better efficiency. Therefore, we need to identify the changes in the phases to identify the best opportunity for reconfiguration.

For this purpose, we developed a technique to detect the change of the program phase by using the data collected from the performance counters. The core of this technique is to leverage an unsupervised learning algorithm, namely k-means clustering, to automatically identify the steady periods of program execution.

The first step of phase detection is data collection. Similar to the application domain detection, we collect the data from the performance monitoring units (PMU). However, there are 53 different counter values in the raw data, and this high dimensionality makes it difficult to further process the data. Therefore, we then apply principal component analysis (PCA) to reduce the dimension of the input and extract the most important information. PCA is a popular feature extraction algorithm that can transform the high dimension input to a low dimension representation with the magnitude of the principal components (PC). It is especially helpful for clustering algorithms since the clustering algorithms suffer from the 'curse of dimensionality' that makes them less effective. We noticed that most of the important information is captured by the magnitude of the first principal component. Figure 16a illustrates the magnitude of the first component of the for all samples in the data collected for the '3mm' (3 consecutive matrix multiplications of different sizes) benchmark in Polybench benchmark suite. The x-axis of the diagram is the index of the sample in time order, and the y-axis is the magnitude of the PC; the red dotted line represents the actual division between phases. As we can see, there are three human-identifiable phases, which correspond to the three matrix multiplications.

However, simply applying PCA is not enough to detect the phases. Notice that the output of PCA has a large number of noise peaks, and these peaks might be identified as separate phases by the unsupervised learning algorithm. Therefore, we apply median filtering to remove the peaks. It replaces the value of a sample with the median within the sliding window, so the large peaks with extreme values will be removed. After applying the filter, as shown in figure 16 (b), the phases can be observed much easier.

Finally, since the phase detection process needs to output logical labels for the phases, we applied the k-Means clustering algorithm to group the data points into clusters where each cluster represents a unique phase. To determine the optimal number of clusters automatically, we applied grid search and use Silhouette score as the criteria, and after this step, clear phases can be detected and are tagged with logical phase label. In figure 16 (c), the y-axis is the logical phase label (the magnitude of it does not have any indication), and we can see that there are three phases which align with the phases that human can identify from figure 16.

4 Results and Discussion

4.1 Phase 1 performance evaluation approach and results

4.1.1 Efficient Architecture Performance Models based on CPU Hardware Performance Monitors

In general, there are two approaches to the problem of performance modeling for future architectures. One is to actually construct the RTL of the design. This is of course highly accurate, including precise estimates of energy and power. Speed of evaluation is variable: one can synthesize into an FPGA (very fast) or perform a software logic-level simulation (very slow) But this approach has very high NRE cost.

The other approach is so-called "cycle accurate" simulation models. These are constructed often from the architect's understanding of the system. Often these are implemented using

event-driven approaches. While they have much lower development time, they are very slow to evaluate.

In Phase 1, we have developed a third approach called a *surrogate model*. Here an application is run on an existing architecture. The performance counters of events relevant to the target architecture are collected during the run. (For example, native DRAM CAS read and write events may be mapped to transactions on the memory bus in the target architecture.) A model is constructed to translate these events into performance and energy estimates of the target architecture. This approach allows a programmer to get virtually instant feedback. Such feedback is vital in enabling applications to be developed in parallel with the target architectures. The relative modeling speed vs. accuracy of these approaches are shown in Figure 17.

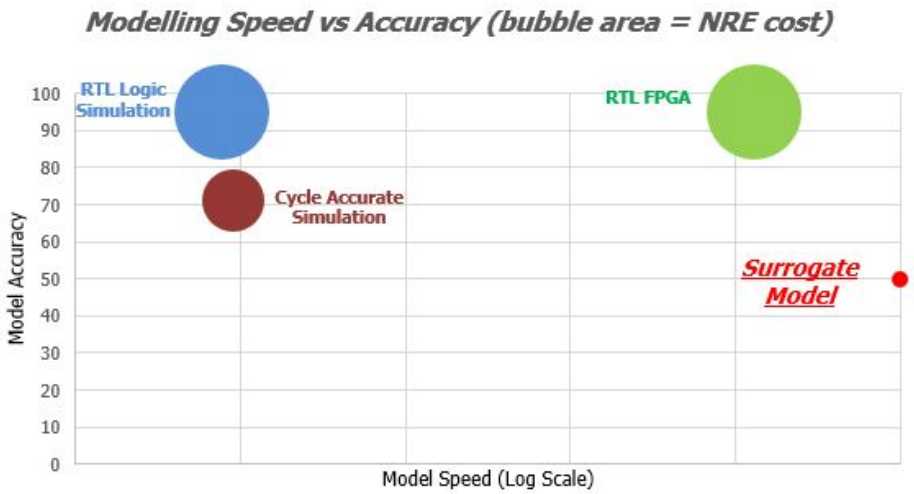

Figure 17: Relative modelling speed vs. accuracy of RTL, cycle accurate and surrogate modeling.

4.1.2 Performance Evaluation for Phase 1 Workflows on Surrogate Model

We developed a tool that uses the hardware performance counters on a native version 4 Xeon Intel processor to record certain events (such as instruction count and lowest level cache miss rate) in order to provide estimates of the run time, cache miss rate and energy on the target TA1 architecture. In our testing, this proved to be within +/- 44%, on average, to the actual numbers from the cycle accurate architecture simulator developed by our TA1 partner.

Using the surrogate model, we were able to demonstrate that Intrepydd (PYDD) significantly improves the estimated energy and execution time relative to Python, as shown in Figure 18. As the geometric mean improvements of the evaluated six workflows, the Intrepydd implementations showed the speedup factor of 130.2 and the energy efficiency factor of 314.1 over the baseline Python implementations.

	GOPS/Watt PYDD	Execution time PYDD (sec)	Total energy PYDD (J)	GOPS/Watt Python	Execution time Python (sec)	Total energy Python (J)	**Execution time speedup factor**	**Total energy Improvement factor**
Workflow Performance								
graphsage	138.1	0.12	0.01	40.3	764.99	113.97	**6481.4**	**22221.5**
ipnsw	21.5	0.43	0.12	26.8	6.56	1.47	**15.2**	**12.1**
recsys	29.1	0.43	0.09	4.0	197.26	294.92	**458.5**	**3325.4**
sinkhorn_wmd	15.0	0.26	0.10	2.1	17.51	49.35	**68.3**	**482.6**
LGC/pr_nibble	49.5	0.05	0.01	113.2	39.41	2.09	**717.1**	**313.4**
LGC/ISTA	14.7	10.84	4.43	4.6	24.13	31.39	**2.2**	**7.1**
convnet	N/A	N/A	N/A	24.0337019	70.79018593	17.67273	N/A	N/A

Figure 18: Comparison of Intrepydd and Python using the surrogate model

Table 2: Benchmark characteristics

Workload	**Domain**	**Description**
bigCLAM	Graph	Overlapping community detection in massive graphs using the BIGCLAM algorithm.
changepoint	Graph	Finds change points of a graph based on node properties
ipnsw	Graph	Non-metric Similarity Graphs for Maximum Inner Product Search
ISTA	ML	Local graph clustering (LGC) through Iterative shrinkage-thresholding
PR-Nibble	ML	Uses the Page Rank algorithm to find local clusters without traversing the entire graph
sinkhorn-wmd	NLP	Computes Word Movers Distance (WMD) using Sinkhorn distances

4.2 Experimental Results on Standard CPUs

In this section, we present an empirical evaluation of our implementation of the INTREPYDD tool chain, which follows the methodology advocated in the SIGPLAN Empirical Evaluation Checklist [18] to the best of our ability. Based on the results and their explanations included below, our claim is that the INTREPYDD approach can deliver notable performance benefits relative to current approaches available to Python programmers for improved performance, namely Cython and Numba; further, these benefits are especially significant for Python applications with execution times that are not dominated by calls to native libraries. We also claim that there is no loss in productivity relative to current approaches, since INTREPYDD's requirement for declaring types of function parameters and return values is also shared by Cython (which imposes additional limitations as well) and by Numba's eager compilation mode. Finally, we claim that INTREPYDD offers more portability than current approaches, since different code versions can be generated from the same INTREPYDD source code using the `host=python` and `host=cpp` modes.

4.2.1 Benchmarks

Given the focus of INTREPYDD on the data analytics area, we picked up two additional workflows, bigCLAM and changepoint from the SDH Workflows. Since the primary contribution

Table 3: Average single core execution times (in seconds) and standard deviation of 10 runs as a percentage of average execution times (in parenthesis) for the baseline Python (times for overall benchmark and primary kernel).

Benchmark	**Python Benchmark times**	**Primary Kernel execution times**
bigCLAM	12.69 (2.25%)	12.36 (1.21%)
changepoint	20.89 (0.71%)	16.37 (0.65%)
ipnsw	21.07 (0.90%)	17.44 (1.61%)
ISTA	30.29 (0.28%)	27.37 (0.06%)
PR-Nibble	53.42 (1.23%)	52.84 (1.18%)
sinkhorn-wmd	48.17 (0.26%)	46.44 (0.08%)

Table 4: Average single core execution times (in seconds) and standard deviation of 10 runs as a percentage of average execution times (in parenthesis) for the primary kernel written in each of Cython, Numba, unoptimized INTREPYDD, and optimized INTREPYDD.

Benchmark	**Cython**	**Numba**	INTREPYDD **(Unopt.)**	INTREPYDD **(Opt.)**
bigCLAM	11.54 (1.31%)	4.157 (0.47%)	2.56 (3.60%)	1.09 (0.89%)
changepoint	119.64 (1.13%)	16.46 (0.48%)	1.47 (0.22%)	1.47 (1.23%)
ipnsw	17.03 (2.43%)	3.21 (0.59%)	1.68 (0.32%)	0.79 (0.18%)
ISTA	26.93 (0.09%)	30.62 (0.10%)	79.36 (0.06%)	18.51 (0.33%)
PR-Nibble	5.04 (0.45%)	3.27 (0.36%)	0.83 (0.84%)	0.006 (0.42%)
sinkhorn-wmd	46.82 (0.20%)	47.03 (0.05%)	47.61 (0.09%)	1.22 (0.40%)

of the current INTREPYDD implementation is to generate improved code, rather than to improve libraries, we expect significant performance improvements primarily for applications with execution times that are not dominated by calls to native libraries. We selected five of these applications for use as benchmarks (bigCLAM, changepoint, ipnsw, PR-Nibble, sinkhorn-wmd). For completeness, a sixth benchmark (ISTA) was also selected which spends significant time in NumPy libraries, even though we do not expect significant performance improvements for such programs.

The benchmarks are summarized in Table 2 and span three different domains in the data analytics area – graph analytics, machine learning, and natural language processing. We are unaware of any single DSL that covers all three domains, where as INTREPYDD can be used for all of them given its broader coverage of the data analytics area.

4.2.2 Experimental Setup

All single-core experiments were performed on a machine with dual Intel Xeon Silver 4114 CPUs with 10 physical cores per CPU socket, running at a constant 2.2 GHz with 192 GB of main memory. Intel Turbo Boost was disabled. Our baseline for benchmark comparison is Python version 3.7.6. All C/C++ code generated by INTREPYDD and Cython (version 0.29.15) was compiled with GCC 7.5.0 using optimization level `O3`. The Numba (version 0.48) and Cython benchmark source codes were written with a programma-

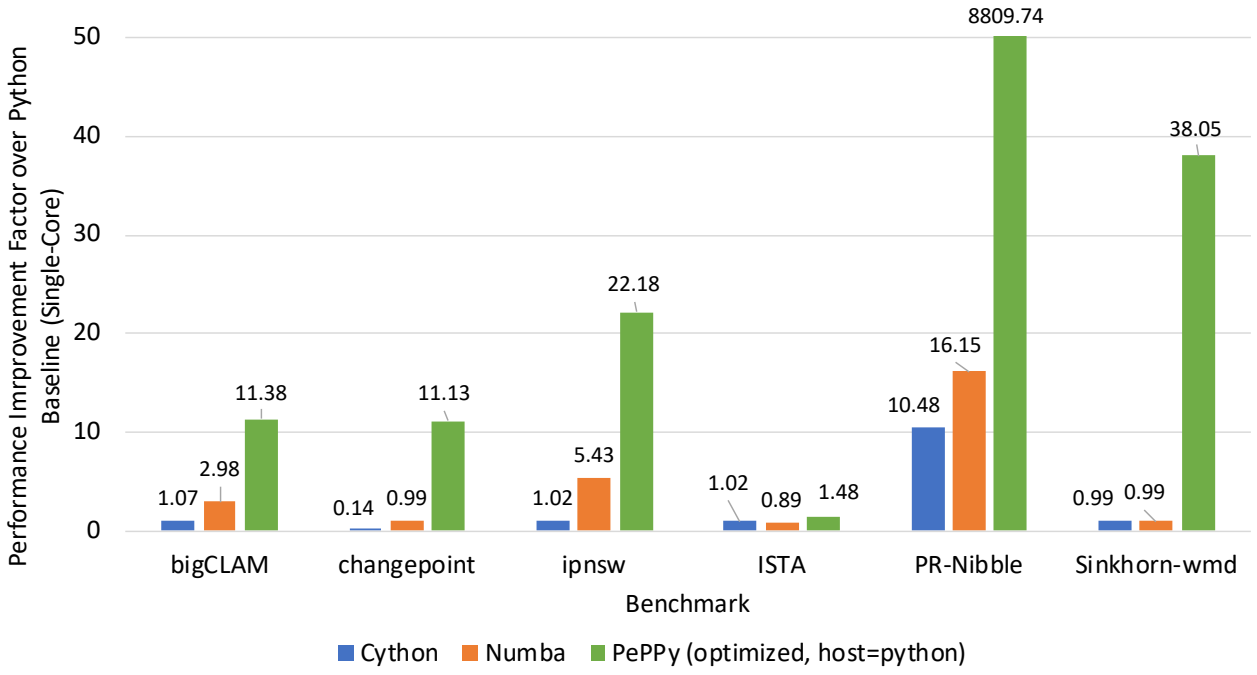

Figure 19: Single core performance improvements for primary kernels relative to Python baseline (derived from data in Tables 3 and 4)

bility similar to that of INTREPYDD, without any additional hand optimizations. For Cython benchmarks, all kernel functions were annotated with `@cython.boundscheck(False)` and `@cython.wraparound(False)`, while for Numba, all functions were annotated with `@jit(nogil=True, nopython=True)`. Each benchmark was compiled once, and executed 11 times (with each run being launched as a new process, which included dynamic optimization only in the case of Numba). The execution times reported for each data point is the average latency of the later 10 runs from the set of 11 (the first run was omitted in the average). The primary kernel execution times were measured at the Python invocation sites, and include any overheads of native function calls. For single core experiments, each process was pinned to a single-core in order to maintain a steady cache state and reduce variations between runs. The normalized standard deviation for the averaged runs varied between 0.06% and 3.60%.

4.2.3 Comparison with Python, Numba, Cython for Single-core Execution

Tables 3 and 4 summarizes the results of our performance measurements of different single-core executions of five versions of each benchmark: baseline Python, Cython, Numba, unoptimized INTREPYDD, and optimized INTREPYDD. The first Python column includes execution times for the entire application so as to provide a perspective on the fraction of the application time spent in its primary kernel, which is reported in all successive columns. All INTREPYDD executions were performed using the `host=python` mode, i.e., they all started with a Python main program which calls the automatically generated code from INTREPYDD as an external library. The optimized INTREPYDD version was obtained by applying the following optimizations, which have been newly developed after the SDH Phase 1.

Table 5: Average single core execution times (in seconds) for the primary Benchmark kernels written in intrepydd and compiled with increasing sets of optimizations: unoptimized, +LICM (Loop-Invariant Code Motion), +Sparse/Dense Array optimizations (Array Operator Fusion), +Memory Allocation Optimizations.

INTREPYDD **Primary Kernel execution times (seconds)**				
Benchmark	**UNOPT**	**+LICM OPT**	**+Array OPT**	**+Memory OPT**
bigCLAM	2.558	2.557	1.541	1.086
changepoint	1.472	1.469	1.466	1.471
ipnsw	1.679	0.786	0.786	0.786
ISTA	79.362	18.732	18.473	18.509
PR-Nibble	0.831	0.114	0.106	0.006
sinkhorn-wmd	47.612	47.395	1.225	1.220

- Loop-Invariant Code Motion (LICM) for standard operators and function calls.
- Dense/Sparse Array Operator Fusion with sparsity optimizations.
- Memory Allocation Optimizations:
  - Reuse an allocated array across multiple array variables; and
  - Access array slices via raw pointers instead of allocating new objects.

As mentioned earlier, the execution times for the five versions are for the primary kernel in each benchmark. The full benchmark time for the baseline Python version is also provided as a reference.

Figure 19 shows the performance improvement ratios for the primary kernels relative to the baseline Python version, using the data in Tables 3 and 4. When compared to baseline Python, the optimized INTREPYDD version shows improved performance ratios between 11.1× and 8809.8× for the five non-library-dominated benchmarks and 1.5× for the library-dominated, ISTA benchmark. These are more significant improvements than those delivered by Cython and Numba, thereby supporting our claim that INTREPYDD delivers notable performance benefits relative to current approaches available to Python programmers. Further, optimized INTREPYDD did not show a performance degradation in any case, though Cython and Numba showed degradations in multiple cases (changepoint and ISTA). We also note from Table 4 that all but one cases of unoptimized INTREPYDD match or exceed the performance of Python. The exception is ISTA, for which the unoptimized INTREPYDD version runs 2.9× slower than the Python version. As mentioned earlier, ISTA is a library-dominated performance, and this gap arises from the fact that the performance of the INTREPYDD libraries have not been tuned like the performance of the NumPy libraries. Finally, the impact of progressively adding the LICM, sparse/dense array optimizations, and memory allocation optimizations is shown in Table 5, and demonstrate that all three optimizations can play significant roles in contributing to performance improvements.

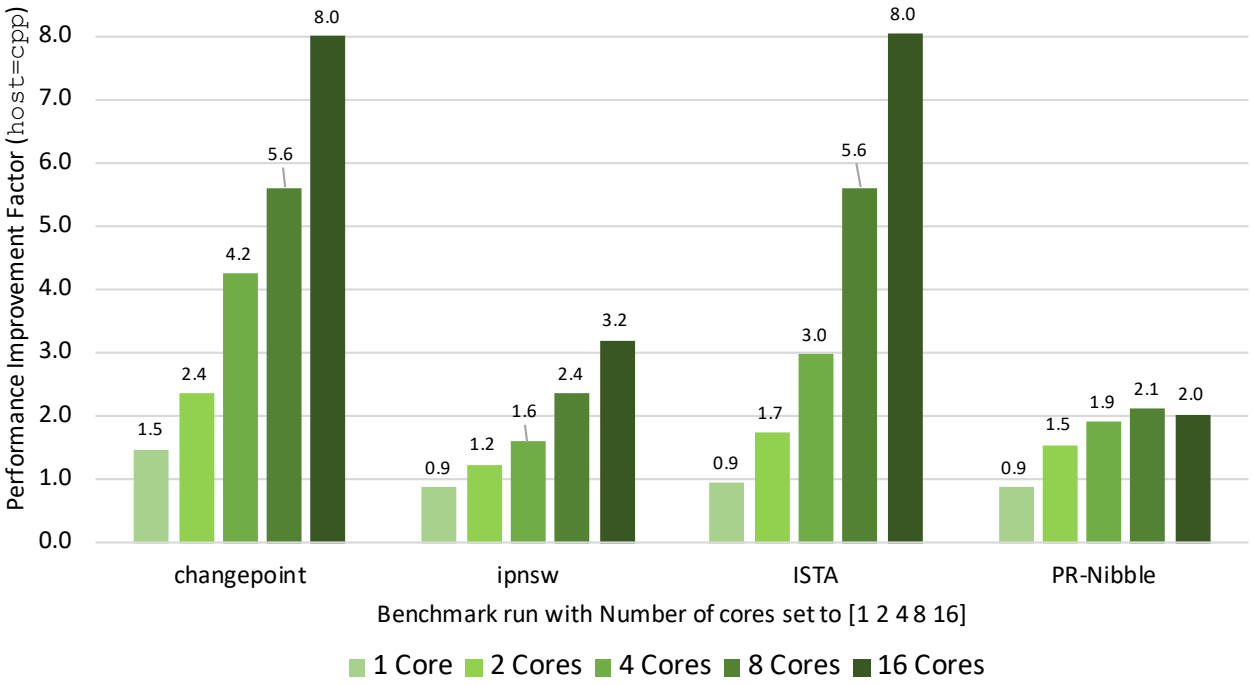

Figure 20: Multi core scalability of INTREPYDD for a subset of the benchmarks in `host=cpp` mode. The Performance Improvement Factor is relative to the single-core execution time in `host=python` mode.

4.2.4 Impact of Parallelization

As mentioned earlier, INTREPYDD supports parallelization in the form of user-specified `pfor` loops with compiler-supported privatization and code generation. Given the known challenges of multithreading within a single Python process, our current INTREPYDD implementation only supports the `pfor` construct in the `host=cpp` mode. In this section, we present results obtained from parallelization of four of the six benchmarks from the previous section that were able to use the `pfor` construct – changepoint, ipnsw, ISTA, and PR-Nibble. In addition to studying the impact of parallelization, the evaluation in this section demonstrates how different code versions can be generated from the same INTREPYDD source code using the `host=python` vs. `host=cpp` modes.

For parallelization experiments, we used a dual socket Intel Xeon E-2680 V4 (14 cores per socket) server running at 2.40 GHz with 128 GB main memory. Intel Hyperthreading and Turbo-boost were disabled. Each benchmark was run using 1, 2, 4, 8 and 16 cores. Since the benchmarks were compiled with `host=cpp` mode, there was no Python code used in these executions. However, as before, the timing measurements were obtained for the primary kernels in the benchmarks following the methodology described in Section 4.2.2.

Figure 20 shows a summary of optimized parallel INTREPYDD `host=cpp` performance compared to single core optimized INTREPYDD `host=python` on 1, 2, 4, 8 and 16 cores. The performance of 1-core `host=cpp` version was observed to be between 0.9–1.8× that of single core `host=python`.

Benchmark	Execution Time (seconds)		
	Python	Julia	INTREPYDD
fibonacci	3.75	0.07	0.06
quicksort	1.76	0.93	0.80
pi-sum	0.57	0.01	0.01
sinkhorn-wmd	46.44	108.60	1.22

Table 6: Average single core execution times (in seconds) for Python, Julia and INTREPYDD versions of four benchmarks.

The benchmarks with outermost level parallelization opportunities (changepoint and ISTA) showed near linear performance scaling with increasing core count; going from a single core performance of 1.5× and 0.9× respectively to 8× over baseline Python when using 16 cores. The ipnsw benchmark also shows performance gains when using more cores. However, the impact of parallelization in this kernel is not as prominent. In the case of PR-Nibble, the performance increases from 0.9× when using 1 core to 2.1× when using 8 cores. However beyond 8 cores, the thread creation overhead exceeds the amount of available work, resulting in a slight slowdown when compared to the 8 core performance.

4.2.5 Comparison with Julia

A comparison against Julia has been provided using micro-benchmarks from Julia's official website [19]. The INTREPYDD versions are directly adapted from the Python versions provided by Julia with additional type annotations. Results (using Julia 1.4.1) for the three non-library dominant benchmarks, i.e. `fibonacci`, `quicksort` and `pi-sum` are shown in table 6.

The micro-benchmark results are comparable to Julia and show negligible performance improvements over Julia. This is attributed to their rather simple nature and the lack of typical complex algebraic expressions that can benefit from INTREPYDD's optimizations. To illustrate the benefits of INTREPYDD's optimizations, the sinkhorn-wmd benchmark was converted to idiomatic Julia. Optimized INTREPYDD shows an order of magnitude improvement over Julia (last row of Table 6).

4.3 Phase 1 SLOC evaluation approach and results

For this evaluation, we compared Intrepydd and (where applicable) Python code for the seven workflows. These were the codes that were input to the CLOC tool (`(http://cloc.sourceforge.net/`) to obtain the SLOC numbers reported in the results spreadsheet. Table 7 summarizes the SLOC sizes for Python and Intrepydd codes for the four non-ML workflows used in the Phase 1 evaluation. The Python codes were obtained from the reference solutions provided by the government team. We also evaluated Intrepydd code fragments for selected kernels from the three ML workflows (convnet, graphsage, recsys), for which no comparable Python code was available because the reference solutions As can be seen from the SLOC results (Table 7) for the non-ML workflows, the Intrepydd and Python SLOC counts are very close for three of the four workflows. The slight increases in SLOC for these three

workflows arises from the addition of type declarations to parameter lists. For the fourth non-ML workflow, ipnsw, the main reason for the larger code size for the Intrepydd version is that, like NumPy, Intrepydd currently does not support C-like multidimensional arrays where different rows can have different lengths. Adding that support in the future will reduce the SLOC gap for ipnsw as well.

Table 7: SLOC of workflows

Workflow	Python SLOC	Intrepydd SLOC
sinkhorn_wmd	10	14
LGC/pr_nibble	25	27
LGC/ISTA	21	27
ipnsw	44	83

As an example, we include below code listings for the Python and Intrepydd versions of the Sinkhorn workflow in Listings 1 and 2.

```
def sinkhorn_wmd_core(K, M, r, x, max_iter, c):
    it = 0
    while it < max_iter:
        u = 1.0 / x
        v = c.multiply(1 / (K.T @ u))
        x = (1 / r) * K @ v.tocsc()
        it += 1
    u = 1.0 / x
    v = c.multiply(1 / (K.T @ u))
    return (u * ((K * M) @ v)).sum(axis=0)
```

Listing 1: Reference Python code for `sinkhorn_wmd` Kernel

```
def sh(K: Array(float64, 2), M: Array(float64, 2),
       r: Array(float64, 2), x: Array(float64, 2), max_iter: int32,
       c_data: Array(float64, 1), c_indices: Array(int32, 1),
       c_indptr: Array(int32,1), c_ncols:int32) -> Array(float64,1):
    c = csr_to_spm(c_data, c_indices, c_indptr, c_ncols)
    it = 0
    while it < max_iter:
        u = div(1.0, x)
        v = c.spm_mul(div(1.0, K.T @ u))
        x = spmm_dense(div(1.0, r).mul(K), v)
        it += 1
    u = div(1.0, x)
    v = c.spm_mul(div(1.0, K.T @ u))
    return mul(u, spmm_dense(mul(K, M), v)).sum(0)
```

Listing 2: INTREPYDD code for `sinkhorn_wmd` Kernel

5 Conclusions

The DDARING project has created software technologies that advances the SDH program goals by developing a novel programming system for generating optimized code variants and optimized hardware configurations for TA1 hardware platforms. Our approach is capable of accelerating workflows for data-intensive analyses to achieve near-ASIC performance, but with the productivity that analysts have come to expect from modern problem-solving environments such as Julia and Python. The components of our approach include a new high-level programming model (Section 3.1), a knowledge base (Section 3.2), a static data-aware optimizer (Section 3.3), a dynamic kernel reoptimizer (Section 3.4), and an auto-tuning and reconfiguration system (Section 3.5). The results of our research have been published in multiple peer-reviewed publications [1–16]. We believe that the technologies developed in the DDARING project will help address many of the portability and productivity challenges associated with future heterogeneous and reconfigurable hardware, and also reshape the way people think about programming in the future.

6 References

[1] Hanqing Zeng, Hongkuan Zhou, Ajitesh Srivastava, Rajgopal Kannan, and Viktor K. Prasanna. GRAPHSAINT: Graph Sampling Based Inductive Learning Method. In *International Conference on Learning Representation*, April 2020.

[2] Piyush Sao, Ramakrishnan Kannan, Prasun Gera, and Richard Vuduc. A supernodal all-pairs shortest paths algorithm for sparse graphs. In *In the Proceedings of the 25th ACM SIGPLAN Symposium on Principles and Practice of Parallel Programming (PPoPP)*, pages 250–261, February 2020.

[3] Hongkuan Zhou, Ajitesh Srivastava, Rajgopal Kannan, and Viktor Prasanna. Design and Implementation of Knowledge Base for Runtime Management of Software Defined Hardware. In *2019 IEEE High Performance Extreme Computing Conference (HPEC 2019)*, September 2019.

[4] Jiajia Li, Bora Uçar, Ümit Çatulyürek, Jimeng Sun, Kevin Barker, and Richard Vuduc. Efficient and effective sparse tensor reordering. In *ACM International Conference on Supercomputing (ICS 2019)*, June 2019.

[5] Piyush Sao, Ramki Ramakrishnan, Xiaoye Li, and Richard Vuduc. A communication-avoiding sparse 3D triangular solve. In *ACM International Conference on Supercomputing (ICS 2019)*, June 2019.

[6] Hanqing Zeng, Hongkuan Zhou, Ajitesh Srivastava, Rajgopal Kannan, and Viktor K. Prasanna. Accurate, Efficient and Scalable Graph Embedding. In *IEEE International Parallel & Distributed Processing Symposium (IPDPS 2019)*, May 2019.

[7] Israt Nisa, Jiajia Li, Aravind Sukumaran-Rajam, Richard Vuduc, and P. Sadayappan. Load-balanced sparse MTTKRP on GPUs. In *IEEE International Parallel & Distributed Processing Symposium (IPDPS 2019)*, May 2019.

[8] Nitish Kumar Srivastava, Hongbo Rong, Prithayan Barua, Guanyu Feng, Huanqi Cao, Zhiru Zhang, Vivek Sarkar, Wenguang Chen, Paul Petersen, Geoff Lowney, Christopher Hughes, Timothy Mattson, and Pradeep Dubey. Productively Generating High-Performance Spatial Hardware for Dense Tensor Computations. In *27th IEEE International Symposium On Field-Programmable Custom Computing Machines (FCCM)*, April 2019.

[9] Pedram Zamirai, Armand Behroozi, and Scott Mahlke. MOODY: Data-Aware Reconfiguration for Energy Efficient Deep Learning. In *First Young Architect Workshop*, February 2019.

[10] Jun Shirako and Vivek Sarkar. Integrating Data Layout Transformations with the Polyhedral Model. In *9th International Workshop on Polyhedral Compilation Techniques (IMPACT 2019)*, January 2019.

[11] Ankush Mandal, He Jiang, Anshumali Shrivastava, and Vivek Sarkar. Topkapi: Parallel and Fast Sketches for Finding Top-K Frequent Elements. In *Advances in Neural Information Processing Systems 31 (NeurIPS)*, December 2018.

[12] Prasanth Chatarasi and Vivek Sarkar. A Preliminary Study of Compiler Transformations for Graph Applications on the Emu System. In *Proceedings of the Workshop on Memory Centric High Performance Computing (MCHPC, co-located with SC18)*, November 2018.

[13] Prithayan Barua, Jun Shirako, and Vivek Sarkar. Cost-driven thread coarsening for GPU kernels. In *27th International Conference on Parallel Architectures and Compilation Techniques (PACT)*, November 2018.

[14] Jonathan Bailey, John Kloosterman, and Scott Mahlke. Scratch That (But Cache This): A Hybrid Register Cache/Scratchpad for GPUs. In *Intl. Conference on Compilers, Architectures and Synthesis for Embedded Systems (CASES)*, pages 2779–2789, October 2018.

[15] Farzad Khorasani, Hodjat Asghari Esfeden, Nael Abu-Ghazaleh, and Vivek Sarkar. In-Register Parameter Caching for Dynamic Neural Nets with Virtual Persistent Processor Specialization. In *The 51st Annual IEEE/ACM International Symposium on Microarchitecture (MICRO)*, October 2018.

[16] Ankush Mandal, Raj Barik, and Vivek Sarkar. Using Dynamic Compilation to Achieve Ninja Performance for CNN Training on Many-Core Processors. In *25th International European Conference on Parallel and Distributed Computing (Euro-Par)*, August 2018.

[17] Polybench/c – the polyhedral benchmark suite.

[18] Sigplan empirical evaluation checklist. http://www.sigplan.org/Resources/EmpiricalEvaluation/, 2017.

[19] Julia micro-benchmarks. https://julialang.org/benchmarks/, 2018.

7 List of Symbols, Abbreviations, and Acronyms

ASIC	Application-Specific Integrated Circuit
BLAS	Basic Linear Algebra Subprogram
CAS	Column Address Strobe
CLOC	Count Lines of Code
COTS	Commercial Off The Shelf
CPP	C Plus Plus (or C++)
CPU	Central Processing Unit
CUDA	Compute Unified Device Architecture
DARPA	Defense Advanced Research Projects Agency
DBSCAN	Density-Based Spatial Clustering of Applications with Noise
DDARING	Dynamic Data-Aware Reconfiguration, Integration and Generation
DNN	Deep Neural Network
DRAM	Dynamic Random Access Memory
DSL	Domain Specific Language
FPGA	Field-Programmable Gate Array
GCC	Gnu C Compiler
GOPS	Giga Operations Per Second
GPU	Graphics Processing Unity
ISTA	Iterative Shrinkage-Thresholding Algorithm
KNN	k Nearest Neighbors
LA	Linear Algebra
LGC	Local Graph Clustering
LICM	Loop Invariant Code Motion
LSTM	Long Short-Term Memory
ML	Machine Learning
NLP	Natural Language Processing
NRE	Non-Recurring Engineering
PCA	Principal Component Analysis
PEP	Python Enhancement Proposal
PI	Principal Investigator
PMU	Performance Monitoring Unit
RNN	Recurrent Neural Network
RTL	Register Transfer Level
SDH	Software Defined Hardware
SGNS	Skip-Gram with Negative Sampling
SIGPLAN	Special Interest Group on Programming Languages
SIMD	Single Instruction Multiple Data
SLOC	Source lines of code
TA1	Technical Area 1
TA2	Technical Area 2